Research Report
492

ANALYSIS OF TIME-INDEPENDENT CONSOLIDATION DATA

by

E. Gregory McNulty
Research Engineer Associate

Thomas C. Hopkins
Research Engineer Chief

and

C. Thomas Gorman
Research Engineer Senior

Division of Research
Bureau of Highways
DEPARTMENT OF TRANSPORTATION
Commonwealth of Kentucky

prepared for publication in the
Proceedings of the
Use of Computers in Geotechnical
Design and Construction
American Society of Civil Engineers
April 25, 1978

in cooperation with
Federal Highway Administration
US DEPARTMENT OF TRANSPORTATION

January 1978

ANALYSIS OF
TIME-INDEPENDENT CONSOLIDATION DATA

by

E. Gregory McNulty,[1] A. M. ASCE

Thomas C. Hopkins,[2] A. M. ASCE

and

C. Thomas Gorman,[3] A. M. ASCE

INTRODUCTION

The one-dimensional laboratory consolidation test developed by Terzaghi permits deformation and drainage only in the vertical direction. The stress-strain characteristics of data obtained from this test are normally studied using a semilogarithmic graphical representation, that is, vertical strain or void ratio is plotted as a function of the logarithm of effective stress. Such a representation permits an analysis of the stress history and compressibility characteristics of soils. Knowledge of these material characteristics is of great practical value in the prediction of settlement associated with loading where the effects of lateral consolidation may be neglected.

Background

The principal event in the stress history of a soil is the maximum vertical stress experienced by the material in its natural subsurface environment. This stress is the result of loads imposed by past or present overlying materials and(or) the result of dessication and is referred to as the "preconsolidation stress." In 1936, Casagrande *(1)* devised an empirical, graphical procedure to determine the preconsolidation stress from the semilogarithmic representation of stress-strain laboratory consolidation data. The essential characteristics of this well known procedure are illustrated in Figure 1.

Before 1955, the compressibility characteristics of particulate materials were expressed as the arithmetic slopes of the line representations of the semilogarithmic, laboratory consolidation curves.

[1]Research Engineer Associate, Soils and Foundations Section, Division of Research, Kentucky Bureau of Highways, Lexington, KY.

[2]Research Engineer Chief, Soils and Foundations Section, Division of Research, Kentucky Bureau of Highways, Lexington, KY.

[3]Research Engineer Senior, Soils and Foundations Section, Division of Research, Kentucky Bureau of Highways, Lexington, KY.

However, these lines did not account for the effects of sample disturbance on the consolidation curves. In 1955, Schmertmann *(7)* developed an empirical, graphical procedure which accounted for the effect of sample disturbance and estimated in situ compressibility characteristics. Figure 1 also shows the essential characteristics of the Schmertmann procedure.

Analyses of stress-strain consolidation data by empirical, graphical techniques such as the Casagrande and Schmertmann constructions have several drawbacks. Terzaghi *(9)* stated that an empirical rule expresses a probability and not a certainty, and to use results obtained by empirical rules without being fully aware of the uncertainties involved is putting oneself at the mercy of the laws of statistics. Similarly, Casagrande believes that the preconsolidation stress should be always considered in terms of a range of values *(2)*. Additionally, the analyses of consolidation data using graphical empirical procedures require considerable amounts of time and effort from competent personnel who oftentimes must make subjective judgements which are susceptible to various graphical ambiguities and computational errors. Results of a survey conducted by Sallfors *(6)* emphasizes these difficulties. Figure 2 shows the scatter in values of the preconsolidation stress P reported by 28 geotechnical engineers who were asked to determine the preconsolidation stress of a given set of stress-strain consolidation data. Results of Sallfors' survey not only show the difficulty involved in determining the preconsolidation stress but also reflect the fact that different methods were used. Sallfors' survey suggested the need to develop some means of alleviating the problems associated with the analysis of stress-strain consolidation data.

Purpose and Scope of Paper

As one step toward minimizing some of the problems associated with the analysis of consolidation data, a computer program was developed which completely reduces, analyzes, and plots time-independent data obtained from three types of laboratory consolidation tests: conventional, controlled-gradient, and controlled-rate-of-strain. Details of the conventional conslidation test are described in ASTM D2435-70. A discussion of the later two testing methods has been presented elsewhere *(2, 3, 8)*. Development of the computer program was prompted by the need for a rapid computational and plotting algorithm which could be used in a data acquisition scheme. The computer program was developed on the IBM 370/165 computer and the Calcomp 663 drum plotter. The program was written in Fortran IV using an algorithm which provides for the mathematical application of the Casagrande and Schmertmann constructions to determine the preconsolidation stress and in situ coefficients of compressibility, respectively. Another innovative feature of the program is the inclusion of two completely different algorithms for selecting the point of maximum curvature.

METHOD OF SOLUTION

The main element of the algorithm is the use of analytical curve-fitting procedures to represent the graphical semilog representation of stress-strain data. An ordinary least-squares polynomial *(10)* is used to represent the compression curve characteristics; a linear least-squares representation is used for the rebound or expansion data. These two functions are applied to the logarithms, base ten, of the abscissae of the data points. In other words, the raw data points which originally spanned logarithmic cycles are reduced to a narrow, arithmetic range of values.

Selection of Curve-Fitting Function

An analytical function used for curve fitting should have the shape characteristics and versatility to accurately duplicate the range of shapes or forms expected from a given type of data representation. Three criteria were considered in selecting a curve-fitting function: functional shape, functional versatility, and functional simplicity. A study of different curve-fitting functions showed that the ordinary polynomial satisfies these requirements amazingly well for the semilog representation of stress-strain consolidation data. Exponential and logarithmic functions were not satisfactory because their seemingly appropriate shapes were found to be too extreme and inflexible to provide an adequate representation of the point of maximum curvature and laboratory virgin compression curve. In contrast, rational functions based on Chebyshev (Tchebycheff) polynomials proved better for fitting the semilog representation of consolidation data than exponential or logarithmic functions. However, rational functions based on Chebyshev polynomials still had the general characteristic of being too inflexible to satisfactorily describe some of the finer, yet essential, shape characteristics. Also, the shape of the rational function was largely dependent on the preselected functional order. In contrast, the ordinary polynomial has less dependence on the functional order used. This is very important from the standpoint of reducing the subjectivity involved in the choice of an appropriate order of the curve-fitting function. Finally, the ordinary polynomial is the simplest of all the curve-fitting functions investigated, and it provides for simpler analytical operations during differentiation and generation of functional expressions. The ordinary polynomial has the form

$$p(x) = c_1 + c_2\, x + c_3\, x^2 + \ldots c_n\, x^{(n\,-\,1)} \qquad 1$$

where $p(x)$ is the given polynomial with terms having constant coefficients c_n for the abscissa terms x with integer powers $(i - 1)$. Derivatives are easily obtained on the ordinary polynomial as follows:

$$d(p(x))/dx = \sum_{i=1}^{n} (i - 1)\, c_i\, x^{(i\,-\,2)}. \qquad 2$$

Limitations of Ordinary Polynomial

The ordinary polynomial does have some important limitations. As noted by Hastings *(4)*, low-degree polynomials have an intrinsic undulatory character that prohibit them from turning sharply and going as straight as sometimes required by curve-fitting considerations. The number of data points as well as the nature of the data impose limitations on the effectiveness of the ordinary polynomial as a curve-fitting function. A few data points (such as obtained from standard consolidation tests) will ambiguously define the semilog representation of the consolidation compression curve. Having too few data points can create two problems. First, a small number of data points will increase the opportunity for greater variation in functional shape characteristics of polynomials of different degrees. Second, there are fewer restraints against the undulatory characteristics of low-degree polynomials. On the other hand, a large number of data points (such as obtained from controlled-gradient and controlled-rate-of-strain consolidation tests) defines the properties of the consolidation compression curve more clearly because the ordinary polynomial is given sufficient information to provide an excellent representation of the data. Also, a greater number of data points avoids the undesirable undulatory characteristics of low-degree polynomials since polynomials of higher degrees can be used.

Mathematical Application of Graphical Constructions

The Casagrande construction is used by the algorithm in the computer program to estimate the probable preconsolidation stress, P_c, and the Schmertmann construction is employed to account for the effects of sample disturbance on the compressibility of the specimen. The major elements in the mathematical application of these two graphical constructions are described below to illustrate the various analytical procedures involved.

Casagrande Construction

The value of P_c as selected by the Casagrande construction is a function of three curve characteristics: the point of maximum curvature, the slope of the curve at the point of maximum curvature, and the selected line representation of the virgin compression curve.

Point of Maximum Curvature

The first step in the Casagrande construction is the selection of the point of maximum curvature (Point O in Figure 1). In the manual application of this step, a subjective decision is made on the basis of the appearance of the manually drawn curve. In the algorithmic application of this step, the point of maximum curvature may be selected by one of two methods. One method employs the mathematical definition of the radius of curvature given in Equation 3, below, and is called the analytical

method. The other procedure is the newly proposed graphical method, which uses the pictorial characteristics of the compression curve to select the point of maximum curvature.

Analytical Method

In the analytical method, the point of maximum curvature is determined from the following mathematical definition:

$$R = (1 + (dy/dx)^2)^{3/2}/(d^2y/dx^2), \quad (3)$$

where dy/dx and d^2y/dx^2 are the first and second derivatives, respectively, of the generated ordinary polynomial (Equation 1) and R is the radius of curvature. The point of maximum curvature is the point on the curve at which R is calculated as a minimum. However, Equation 3 cannot be used directly to select the visual point of maximum curvature from the analytical expression generated by the polynomial fit of the compression data. The difficulty involved is illustrated in Figures 3a and 3b. The circle in Figure 3a is drawn on x and y axes having the same scales. A unique analytical or visual point of maximum curvature does not exist on the circle in Figure 3a. However, if the x and y axes have different scales as shown in Figure 3b, there are two discrete visual points of maximum curvature, a and b, while an analytical point of maximum curvature still does not exist when Equation 3 is used. This distortion is caused by different scales in plotting and must be accounted for before the visual point of maximum curvature can be analytically selected using Equation 3 (see the Appendix).

For Equation 3 to apply to a graphical representation of an analytical function, the horizontal and vertical axes used in plotting the analytical function must have the same scale. When the fitted curves are plotted on axes which do not have the same scale, a correction factor must be included in Equation 3 to modify the derivatives so that they reflect the actual visual distortion caused by the scale difference. Since strain and logarithm of effective stress are dimensionless quantities, the correction factor is expressed simply as the ratio of horizontal scale to vertical scale as follows:

$$\text{FACTOR} = \text{HORIZONTAL SCALE/VERTICAL SCALE} \quad (4)$$

This correction factor is to Equation 3 in the following way to make the analytical and visual points of maximum curvature the same:

$$R = (1 + ((dy/dx)\ (\text{FACTOR}))^2)^{3/2}/((d^2y/dx^2)(\text{FACTOR})) \quad (5)$$

Graphical Method

Because the analytical method may not always be successful in determining the point of maximum curvature on curves having ill-defined curvature, the graphical method was developed. In this method, the recompression and virgin compression curves are idealized as straight-line segments which are connected by a transitional curve. Several assumptions are made. First, the recompression curve is assumed to have the same slope as the rebound curve as shown in Figure 4. The Schmertmann construction employs

a similar assumption. Second, the transitional curve lying between the two straight-line segments is assumed to be smooth and evenly distributed. Consequently, the point of maximum curvature is at the center of this transitional curve. Finally, the center point of the transitional curve is found by bisecting the interior angle formed by the intersection of the line representations of the recompression and virgin portions of the compression curves to obtain the point of maximum curvature as shown in Figure 4.

Implementation of the graphical method consists of the following steps as shown in Figure 4:

1. A line having the same slope as the rebound curve is drawn tangent to the recompression curve.

2. The virgin compression curve is then represented by a line having the slope of its straight portion.

3. The tangent of the recompression curve and the straight-line representation of the virgin compression curve are extended until they intersect.

4. The interior angle formed by the intersection of those two lines is bisected.

5. The angle bisector is then extended until it intersects the compression curve. This point of intersection is selected as the point of maximum curvature.

If the point of maximum curvature can be computed by Equation 5, the point selected by the graphical method may be located slightly before or after the analytically selected point of maximum curvature. The location of the graphically selected point relative to the analytically selected point depends on how the shape of the transitional curve deviates from the assumption of a smooth and evenly distributed curve. When the data do not precisely define where the fitted transitional curve should have its point of maximum curvature, only an estimate is possible. The point selected by the graphical method is a reasonably good estimate of the point of maximum curvature.

After the point of maximum curvature is selected, the Casagrande procedure is completed by determining the equations of the horizontal, tangential, and angle-bisector lines which intersect at the selected point of maximum curvature on the fitted polynomial. The first derivative of Equation 2 is used to establish the slope of the tangential line at the point of maximum curvature. The equations of the horizontal line and angle bisector are established from simple geometrical considerations. The final step in the mathematical application of the Casagrande construction comes in the selection of the line representation of the virgin compression curve and its intersection with the angle bisector line, OC, in Figure 1. The line representation of the virgin compression curve is selected from the polynomial representation of the compression data points. To select the most appropriate straight-line representation of the virgin compression curve, the portion of the fitted polynomial which is steep and has a relatively constant slope is used. To do this, a percent-difference criterion is used. If the slope is relatively constant, the percent difference between slopes of consecutively generated search points will be very small and

that portion of the curve will be nearly a straight line. When the percent-difference criterion of 0.02 percent is satisfied, that portion of the curve is used to produce the straight-line representation of the laboratory virgin compression curve. After the laboratory virgin compression line has been selected, the probable preconsolidation stress, P_c, is determined at the intersection point of this line with the angle bisector line by taking the antilog of the abscissa at the point of intersection.

Schmertmann Construction

After the Casagrande construction, the Schmertmann construction is mathematically applied. The first step in this procedure is to construct the in situ recompression curve as shown by line XY in Figure 1. The in situ recompression curve is represented by a line passing through the in situ state of stress and strain at point X having the same slope, SR, as the rebound curve, EF. Next, the in situ, virgin compression curve is represented by a line passing from the recompression line at the preconsolidation stress, point Y, to the point where the virgin curve intersects the ordinate value of strain at 42 percent of the initial void ratio, point Z in Figure 1. Finally, a minimum preconsolidation stress, P_c (MINIMUM), is determined in accordance with a procedure modified by Schmertmann *(7)*. The minimum preconsolidation stress is found simply by extending the laboratory virgin curve until it intersects either the $\epsilon_v = 0$ line (underconsolidated material) or the in situ recompression line, XY, as shown in Figure 1.

Influence of the Degree of Polynomial

In the mathematical application of the Casagrande and Schmertmann graphical constructions, the influence of the degree of polynomial has a range of effects on the selection of the point of maximum curvature and the line representation of the virgin compression curve, and hence the determined values of the probable preconsolidation stress, P_c, and in situ compression ratio, CR ($CR = C_c/(1 + e_o)$). The influence of the preselected degree of polynomial is least when the consolidation compression curve is well defined; that is, one which has a well-defined point of maximum curvature and a reasonably straight virgin compression curve. Generally, but not always, this is the case when the compression curve is defined by a sufficient number of data points (such as obtained from the controlled-gradient and controlled-rate-of-strain consolidation tests). The greatest effect of degree of polynomial occurs when the compression curve is ambiguously or ill defined; that is, where there is considerable uncertainty in selecting the location of the point of maximum curvature and straight portion of the virgin compression curve. This condition usually arises in cases where there are fewer than eight data points defining the consolidation compression curve, as is usually the case with the standard consolidation test. Three isolated examples are given below to illustrate that the influence of degree of polynomial depends to a large

extent on the uncertainty involved in selecting the point of maximum curvature and straight portion of the virgin compression. These three examples are by no means all inclusive.

An example of a well-defined consoldiation curve is shown in Figure 5. The data were obtained from controlled-gradient consolidation test (CG-13) and analyzed using both the analytical and graphical methods. To illustrate the effect of the choice of the degree of polynomial on the computed values of P_c and CR, the data given in Figure 5 were analyzed using polynomials of different degrees and the results are shown in Figures 6 and 7. If the graphical and analytical methods are considered separately, fairly consistent values of P_c and CR are obtained for polynomial degrees of six or greater. Also, Figures 6 and 7 indicate that, when a large number of data points are available, the highest possible degree (equal to eleven in the computer program) should be used to obtain fairly accurate values of P_c and CR.

An example intermediate between a well-defined and ambiguously-defined consolidation compression curve is shown in Figures 8 and 9 (Standard Test 24) for both the analytical and graphical methods. Although the straight portion of the virgin compression curve is sufficiently well defined, these data are considered to be an intermediate example because there is a reasonable amount of ambiguity in the location of the point of maximum curvature. Consequently, the influence of degree of polynomial on the results shown in Figures 8 and 9 is more pronounced than the example in Figure 5 because the few data points do not completely define the location of the point of maximum curvature. When dealing with few data points, experience has shown the best preselected degree of polynomial is equal to the number of data points minus two. Figures 10 and 11 indicate that the least-squares smoothing incurred with polynomial degrees slightly less than the maximum possible degree provides reasonably consistent values of P_c and CR when either method is used.

Finally, an example of an ambiguously-defined consolidation curve is illustrated in Figures 12 and 13. The consolidation curve is considered to be ambiguously-defined because of the great ambiguity in the location of the point of maximum curvature and lack of a definite straight portion in the virgin compression curve. The considerable ambiquity in the location of the point of maximum curvature is due to the nature of the data. In considering the influence of polynomial degree, differences between the determination of the point of maximum curvature by the analytical and graphical methods must be considered. The selection of the point of maximum curvature by the analytical method (Equation 5) is greatly affected by the degree of polynomial because small changes in the fitted curve overshadow the ambiguous information furnished by the data points describing the location of the point of maximum curvature. This result can be noted by comparing the determined values for P_c and CR in Figures 12a and 12b. In contrast, the effect of polynomial degree on the determined values of P_c and CR is less

significant when the point of maximum curvature is determined by the graphical method (Figure 4). This result can be seen by comparing the values for P_c and CR in Figures 13a and 13b. Any effect of polynomial degree on the selection of the point of maximum curvature can be expected to have a corresponding effect on the determined values of P_c and CR. This problem of selecting the point of maximum curvature on curves having ill-defined curvature is an example of where the use of empirical, graphical procedures to determine the properties of stress-strain consolidation data may be limited. In addition, questions may even arise concerning their applicability to the analysis of certain types of data. With this in mind, the validity of the graphical method as opposed to the analytical method to determine the point of maximum curvature on data curves similar to the ones for the Standard Test 12 in Figures 13a and 13b is a matter of individual judgment.

Program Output

Figures 5, 8, 9, 12, and 13 are examples of plotted output from the computer program. These plots show data points, fitted curves, numerical results, and all the steps involved in the graphical analyses.

CONCLUSIONS

1. The computerized version of this program has proven effective in the reduction analysis of stress-strain data obtained from more than 40 controlled and 30 standard consolidation tests.
2. The program is a valuable aid in rapidly analyzing data from a large number of consolidation tests, particularly ones producing large amounts of data such as the controlled-gradient and controlled-rate-of-strain consolidation tests.
3. The program is a suitable adjunct to any data acquisition scheme involving stress-strain consolidation data.
4. The program can be readily adapted for use with cathode-ray plotters such as the Tektronix Model 4012 or any other peripheral computer equipment that is compatible with the IBM 370/165 computer.
5. A graphical procedure to select the point of maximum curvature has been proposed and included in the algorithm of the computer program. This graphical method is generally less susceptible to small variations in the fitted polynomial than the analytical method which uses Equation 5 and can be used when data are reduced manually.
6. The effectiveness of the algorithm depends on two things: the applicability of the Casagrande and Schmertmann constructions and the adequacy of the curve representation of the data by the ordinary polynomial.
7. The best-curve representation of the data is usually obtained when the highest degree of polynomial which provides some least-squares smoothing is used.

8. Sallfors *(6)* has pointed out that it is possible to represent the compression data with a number of different curves where there are only six or seven data points. This type of variation accounts for most discrepancies between values of P_c and CR for representations of standard consolidation compression curves. For controlled-gradient consolidation test data, the greater amount of data greatly reduces the variation in results for different polynomial degrees.
9. The location of the point of maximum curvature is dependent on the plotted representation of an analytical curve. Hence, values determined for P_c can be significantly affected by the scales to which the semilog, stress-strain consolidation curves are plotted.

NOTATION

CG	Controlled-gradient consolidation test
C_c	Compression index
CR	Compression ratio
DEG	Degree of polynomial fit
ϵ	Vertical strain, percent
EC	Vertical preconsolidation strain
EO	In situ void ratio
e_o	In situ void ratio
OCR	Overconsolidation ratio
P_c	Preconsolidation stress
PC	Preconsolidation stress
PO	In situ vertical stress

σ_v' Vertical effective stress

STD Standard consolidation test

SR Swell Ratio

REFERENCES

1. Casagrande, A.; *The Determination of the Preconsolidation Load and Its Practical Significance,* **Proceedings,** First International Conference on Soil Mechanics and Foundation Engineering, Cambridge, MA, Vol 3, 1936, pp 60-64.
2. Casagrande, A.; Personal communication with E. G. McNulty, Harvard University, August 18, 1975.
3. Gorman, C. T.; *Constant-Rate-of-Strain and Controlled-Gradient Consolidation Testing,* Division of Research, Kentucky Bureau of Highways, May 1976.
4. Hastings, C.; Woodward, J. T.; and Wong, J. P., Jr.; **Approximations for Digital Computers,** Princeton University Press, Princeton, NJ, 1955.
5. Lowe, III, J.; Jonas E.; and Obrician, V.; *Controlled Gradient Consolidation Test,* **Journal of Soil Mechanics and Foundations Division,** American Society of Civil Engineers, Vol. 95, No. SM1, Paper No. 6327, January 1969, pp 77-97.
6. Sallfors, G.; *Preconsolidation Pressure of Soft, High Plastic Clays,* thesis presented to Chalmers University of Technology, Goteborg, Sweden, in partial fulfillment of the requirements for the degree of Doctor of Philosophy, October 1975.
7. Schmertmann, J. H.; *The Undisturbed Consolidation Behavior of Clay,* **Transactions,** American Society of Civil Engineers, Vol 120, Paper No. 2775, 1955, pp 1201-1227.
8. Smith, R. E.; and Wahls, H. E.; *Consolidation under Constant Rate of Strain,* **Journal of the Soil Mechanics and Foundation Division,** American Society of Civil Engineers, Vol 95, No. SM2, Paper No. 6452, March 1969, pp 319-539.
9. Terzaghi, K. B., **Theoretical Soil Mechanics,** John Wiley and Sons, Inc., New York, 1943.
10. Thrailkill, L.; Allen, K.; and Taylor, W.; *Numerical Analysis Library for University of Kentucky 370,* University of Kentucky, Lexington, KY, December 1970, pp 70-71.

APPENDIX

Dependency of Point of Maximum Curvature on Plotting Scales

The location of the visual point of maximum curvature is influenced by the way in which the plotting axes are scaled when any analytical curve is drawn. When the effects of the plotting scales are ignored, as in case of Equation 3, Figure 14 shows how the selected point of maximum curvature will not coincide with the visual point of maximum curvature selected in Figure 5a. When Equation 3 is used, the disparity between the selected and visual points of maximum curvature is usually much greater with the point of maximum curvature being selected in the straight portion of the virgin compression curve. Consequently, the benefits of using Equation 5 as compared to Equation 3 are obvious when the results of Figures 5a and 14 are compared.

A geometrical approximation has been developed by the principal author of this paper as an alternate way of determining the radius of curvature, and consequently, the point of maximum curvature. This geometrical approximation will constitute a proof that the location of the visual point of maximum curvature is greatly affected by the scaling of any analytical curve because this geometrical method yields the same results as obtained from Equation 5. The basic steps associated with this geometrical approach are shown below in reference to Figure 15:

1. Points A and B are selected distance dx apart on the fitted polynomial curve.
2. Tangents, A1 and B1, are drawn at points A and B.
3. Normals, A2 and B2, are drawn perpendicular to tangents A1 and B1 at points A and B, respectively, and extended until they intersect at point P.
4. Point O is located on the curve halfway between points A and B.
5. Line OP is drawn and its length measured and used as an approximate value of the radius of curvature at point O.

Figure 16 demonstrates the computerized operation of the geometrical approach to determining values for the radius of curvature at points along the fitted polynomial given in Figure 5a. Figure 17 shows the close comparison between values of the radius of curvature determined by this geometrical approach and by Equation 5. It is easy to see that both methods yield the same minimum value for the radius of curvature at the same point on the fitted polynomial curve.

The fact that the location of the visual point of maximum curvature depends on the effects of the plotting scales is more clearly shown through a discussion of the computer application of the geometrical approach to determining values of the radius of curvature. The key point in understanding the effects of scaling on the location of the visual point of maximum curvature is recognizing how

these effects must be accounted for so that the normals of the geometrical approximation are **plotted** perpendicular to the **plotted** polynomial.

The mathematical identity describing the relationship between two perpendicular lines is

$$M_2 = -1/M_1 \qquad 6a$$

or

$$M_1 M_2 = -1, \qquad 6b$$

where M_1 is slope of the tangent and M_2 is the slope of the perpendicular to the tangent. However, a normal will not be plotted perpendicular to a plotted line if the identity in Equation 6 is used when the scales of the horizontal and vertical plotting axes are different. Figure 18a shows the relationship between two perpendicular lines when the scales of the plotting axes are the same; Figure 18b illustrates what occurs when the scales are not the same on both plotting axes. In Figure 18b, the horizontal scale is proportioned so that there are 0.300 units per inch of horizontal plotting distance (i.e. three log cycles over 10 inches); the vertical scale is graduated for 0.02 units per inch of vertical plotting distance. Normals will be **plotted** perpendicular to the **plotted** line only if the slope of the plotted line is corrected for the effects of the plotting scales. This is accomplished by modifying the value of slope for line one, M_1, in Figure 18a, using a correction factor that converts the vertical and horizontal components, dy and dx, respectively, into the actual vertical plot distance in inches for a given number of inches in the horizontal direction. For instance, M_1 can be expressed as follows:

$$M_1 = dy/dx. \qquad 7$$

To convert the vertical and horizontal components, dy and dx, respectively, into their actual plotting distances, simply divide each component by the scaling values used to express the number of units for an inch of plot in both the horizontal and vertical directions. From Figure 18b, scaling values of 0.300 and 0.02 are applied to the horizontal and vertical directions, respectively. Therefore, it follows that

$$(dy/0.02)/(dx/0.300) = 15dy/dx, \qquad 8$$

where 15 is the value of the correction factor needed to reflect the actual plotting distances involved. This correction factor, FACTOR, can be expressed as

$$\text{FACTOR} = \text{HORIZONTAL SCALE/VERTICAL SCALE.} \qquad 9$$

The modified value of slope, M_1*, can be expressed in terms of the slope M_1 as

$$M_1^* = \text{FACTOR} \cdot M_1, \qquad 10a$$

or

$$M_1 = M_1^*/\text{FACTOR}. \qquad 10b$$

To obtain the slope of the normal, M_2, which will make the plotted normal appear perpendicular

to the line having a slope M_1, the modified normal slope M_2*, must first be obtained using the identity given in Equation 6 as follows:

$$M_2^* = -1/M_1^* \quad (11a)$$

or

$$M_2^* = -1/(M_1 \cdot \text{FACTOR}). \quad (11b)$$

The slope of the normal, M_2, is obtained by removing the correction factor from the visual slope M_2* as follows:

$$M_2 = M_2^*/\text{FACTOR} \quad (12a)$$

or

$$M_2^* = M_2 \cdot \text{FACTOR}. \quad (12b)$$

Next, the mathematical relationship is derived between the tangent and normal slopes, M_1 and M_2, when the effects of scaling are considered. Solving for the term M_1 from Equation 11b yields

$$M_1 = -1/(\text{FACTOR} \cdot M_2^*) \quad (13)$$

Substituting the relationship for M_2* from Equation 12b into Equation 13 yields

$$M_1 = -1/(\text{FACTOR} \cdot \text{FACTOR} \cdot M_2) \quad (14)$$

Rearranging,

$$M_1 M_2 (\text{FACTOR})^2 = -1. \quad (15)$$

Figure 19 provides an illustration of where this procedure was followed. The value of FACTOR as computed by Equation 9 is 15 for the horizontal and vertical scales provided. Substituting the values of FACTOR and slopes M_1 and M_2 from Figure 19 into Equation 15 yields

$$(-0.06667)\ (0.06667)\ (15)^2 = -1. \quad (16)$$

Finally, the squaring of the term FACTOR in Equations 15 and 16 implies that the visual point of maximum curvature is a function of the square of the term FACTOR. Referring to Equation 5, this inference is confirmed. The radius of curvature R, as given by Equation 5, may be expressed in terms of FACTOR as follows:

$$R \propto ((\text{FACTOR})^2)^{3/2}/\text{FACTOR}, \quad (17a)$$

which reduces to

$$R \propto (\text{FACTOR})^2. \quad (17b)$$

Therefore, the effect of scaling on the location of the visual point of maximum curvature is proportional to the square of the correction factor, FACTOR.

This result has many practical ramifications. For instance, Figures 20a and 20b illustrate two plots where the number of log cycles for a given horizontal distance are different. In Figures 20a and 20b, there are two and five log cycles, respectively, plotted over a horizontal distance of 10 inches. The

value of FACTOR in Figures 20a is 10 and fixes the visual point of maximum curvature at the abscissa value for 6.9 Tsf. In Figure 20b, FACTOR is equal to 25 and locates the visual point of MAXIMUM curvature at the abscissa value for 5.22 Tsf. Hence, these two figures demonstrate that the scales to which consolidation data are plotted, and therefore the magnitude of FACTOR, has a significant effect on the location of the visual point of maximum curvature. The effects of a wide range of values of FACTOR on the abscissa location of the visual point of MAXIMUM curvature are illustrated in Figure 21. Usually, the value of FACTOR lies somewhere between a value of 1 and 100. This is the range where the influence of scaling is greatest, as shown by Figure 21. The value of FACTOR can be changed in another way by expanding the length of the vertical plotting axis to express fewer units of strain per inch for a given horizontal scale. This increases the value of FACTOR and causes the visual point of MAXIMUM curvature to be shifted to higher abscissa values located to the right on the compression curve. A decrease in the value of FACTOR causes the visual point of maximum curvature to be shifted to lower abscissa values located to the left on the compression curve. Both of these facts can be inferred from Figure 21. Although Figure 21 applies specifically to the data which appears in Figure 20, similar trends will be obtained for any other semi-logarithmic representation of stress-strain consolidation data.

ACKNOWLEDGEMENT

This report was prepared as a part of Research Study KYHPR-75-74, Controlled Rate of Strain and Controlled Gradient Consolidation Testing, HPR-PL-1(13), Part II. The study is sponsored jointly by the Kentucky Bureau of Highways and the Federal Highway Administration, US Department of Transportation. The report does not necessarily reflect the views of the Kentucky Bureau of Highways nor the Federal Highway Administration.

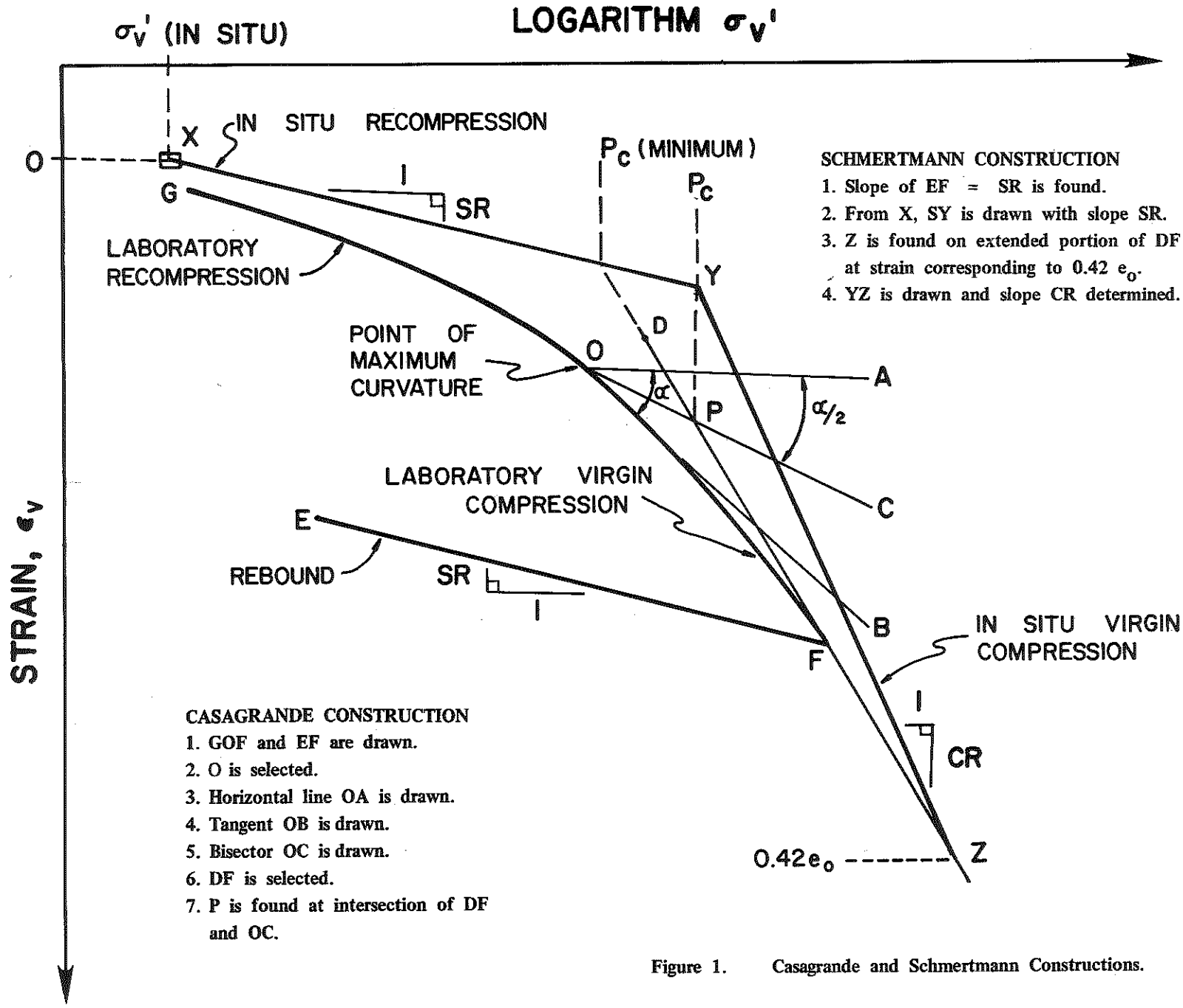

Figure 1. Casagrande and Schmertmann Constructions.

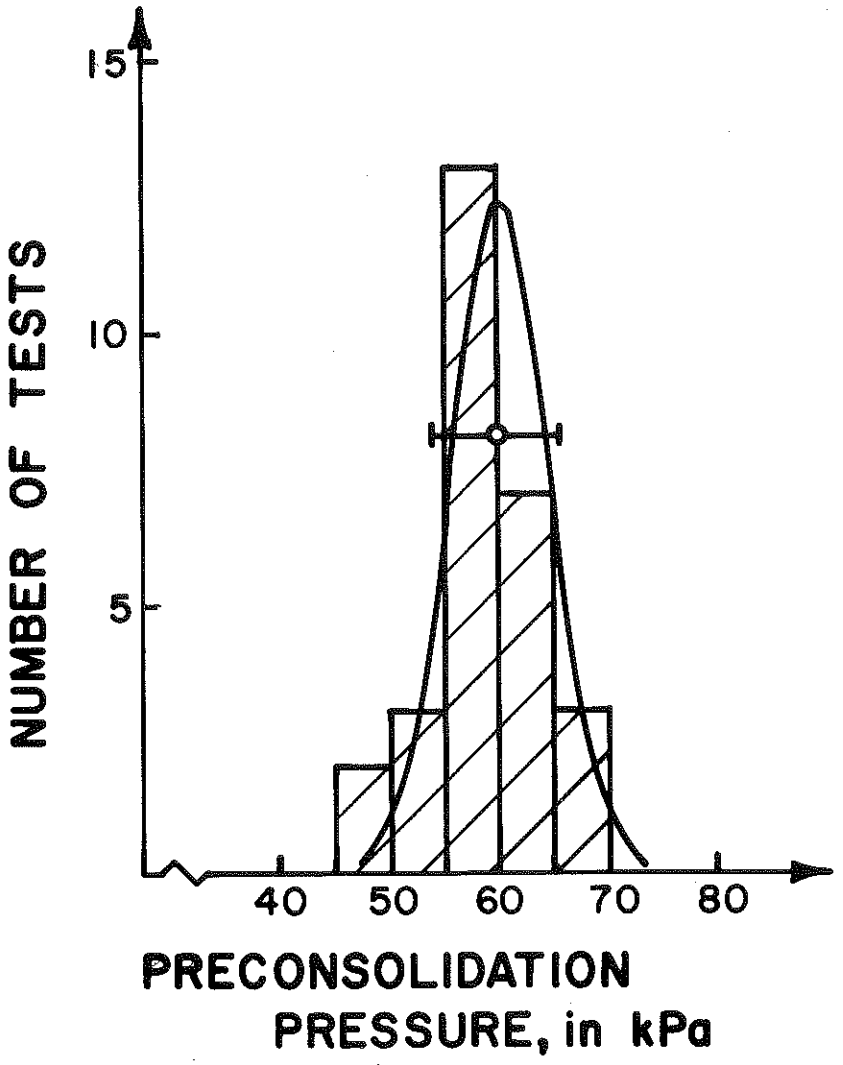

Figure 2. Distribution of Evaluated Preconsolidation Pressures (80-percent confidence interval) (after Sallfors, 1975).

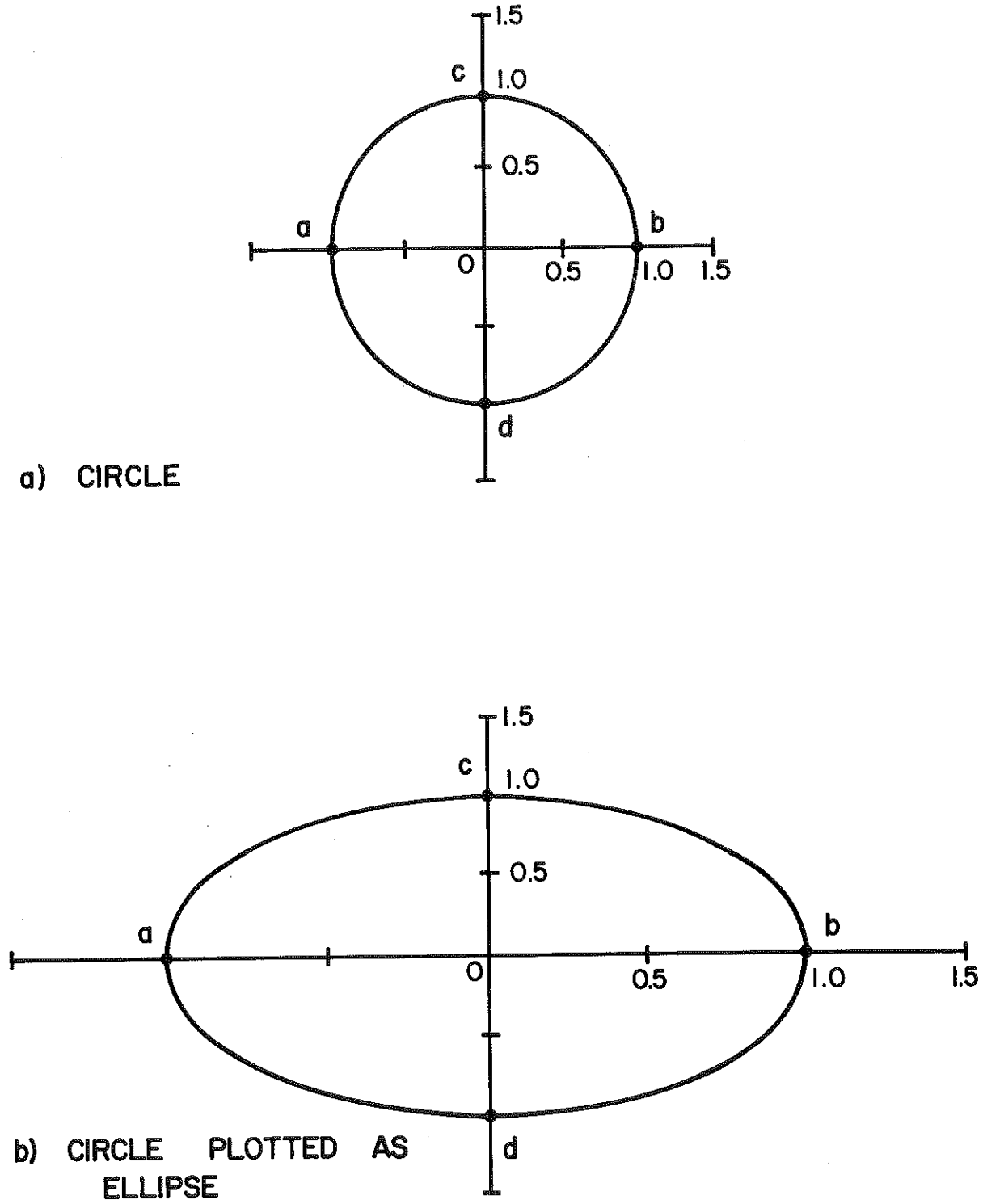

Figure 3. Illustration of Distortional Effects Caused by Different Plotting Scales when Considering Visual Points of Maximum Curvature.

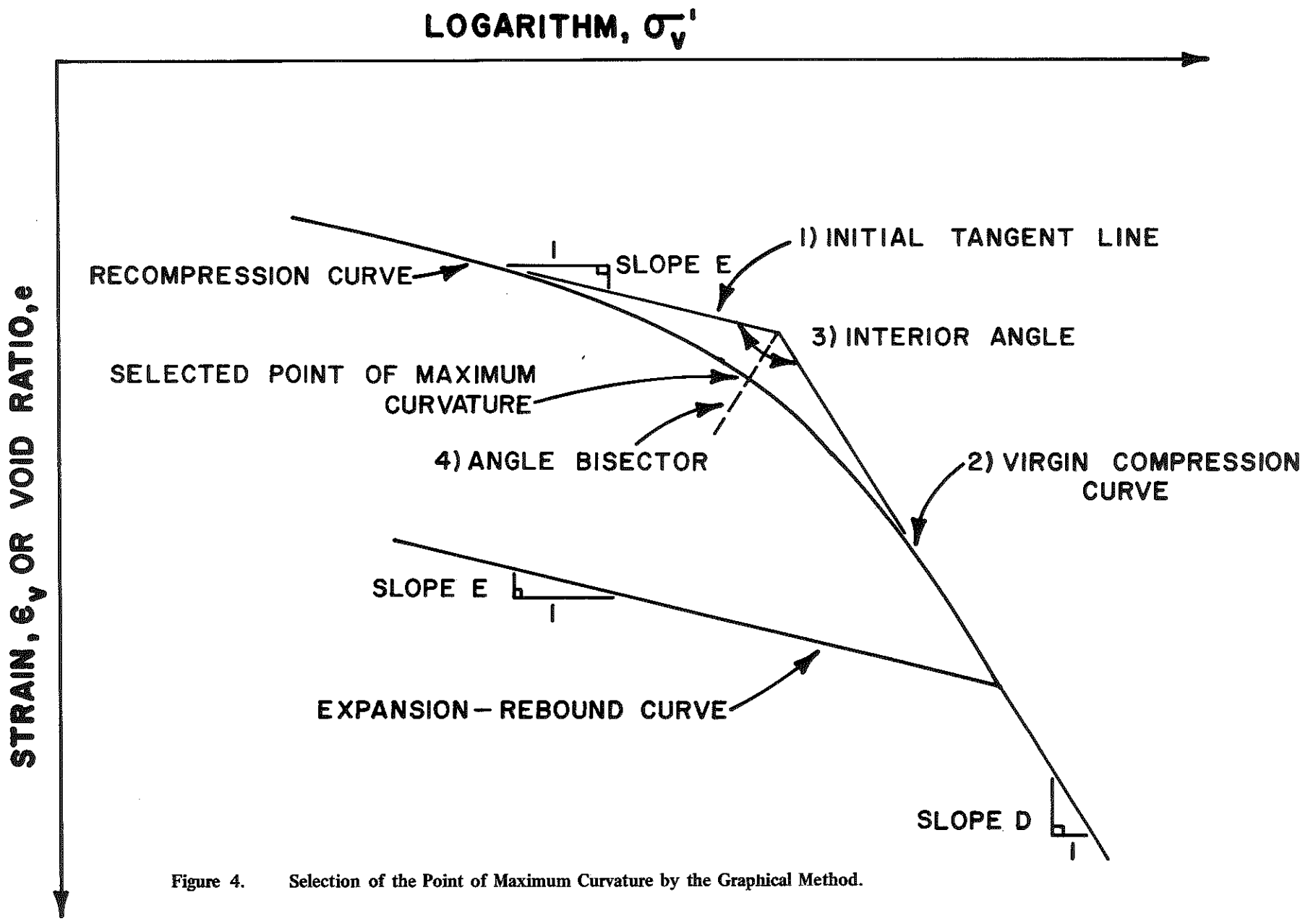

Figure 4. Selection of the Point of Maximum Curvature by the Graphical Method.

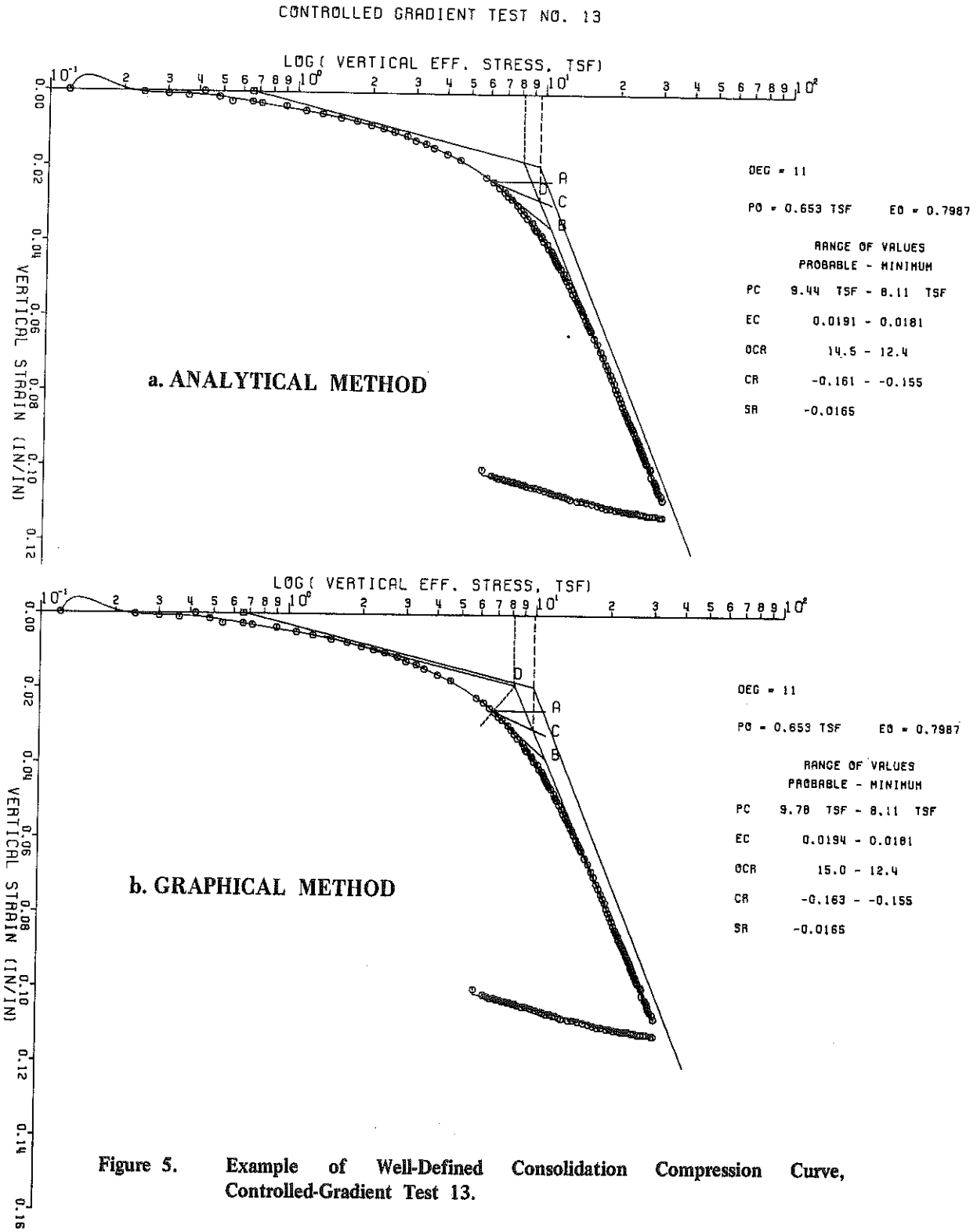

Figure 5. **Example of Well-Defined Consolidation Compression Curve, Controlled-Gradient Test 13.**

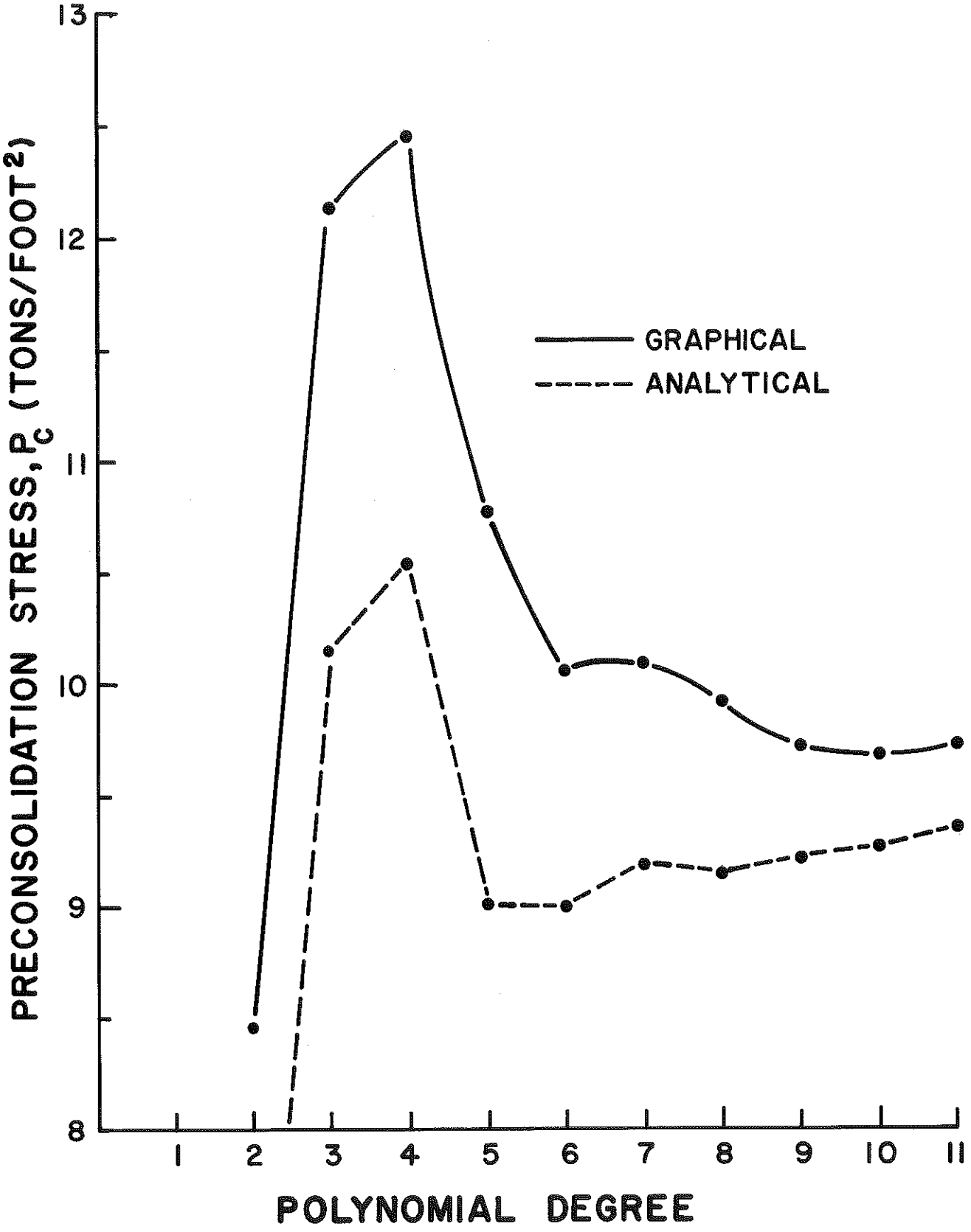

Figure 6. Preconsolidation Stress versus Polynomial Degree, Controlled-Gradient Test 13.

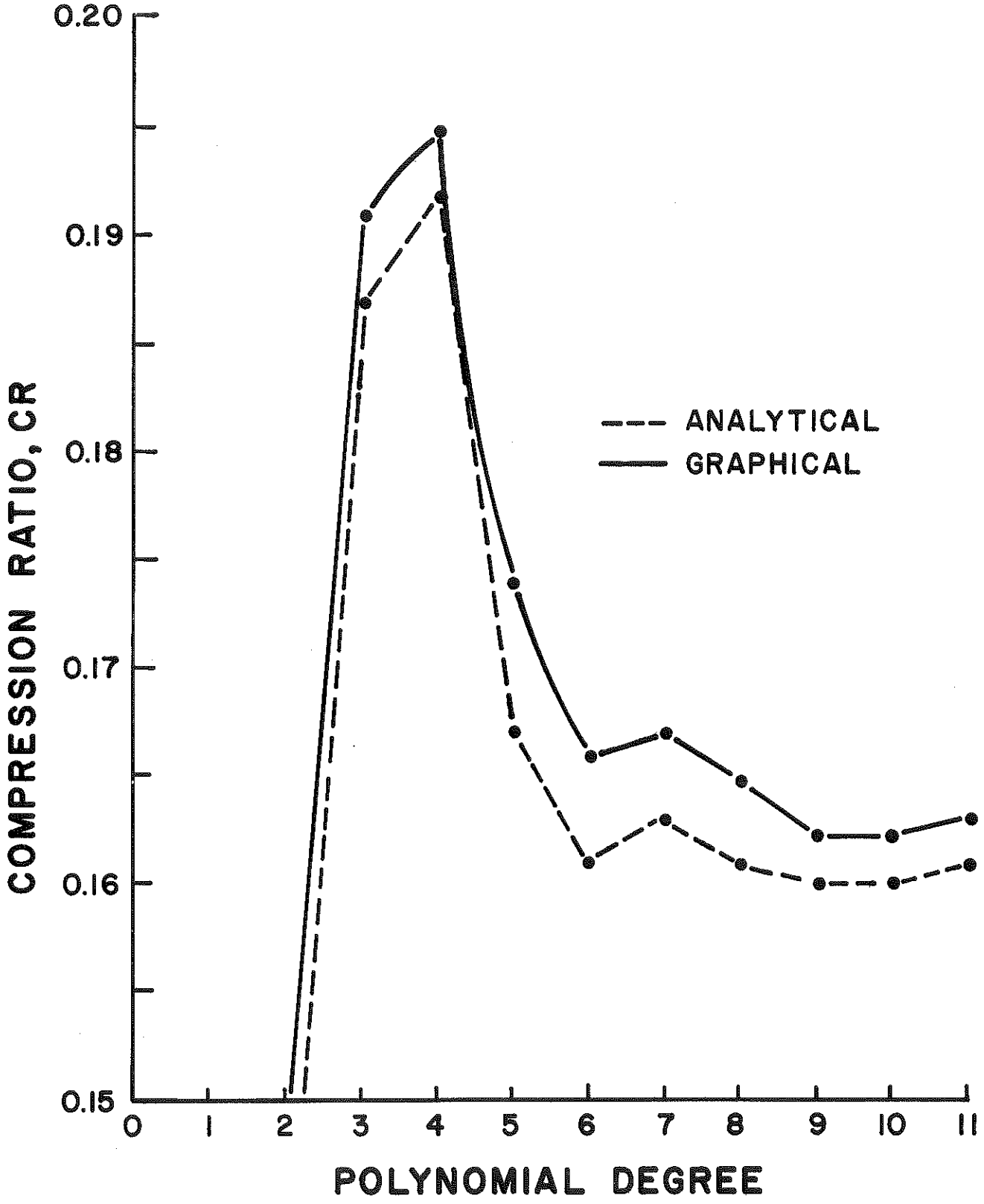

Figure 7. Compression Ratio versus Polynomial Degree, Controlled-Gradient Test 13.

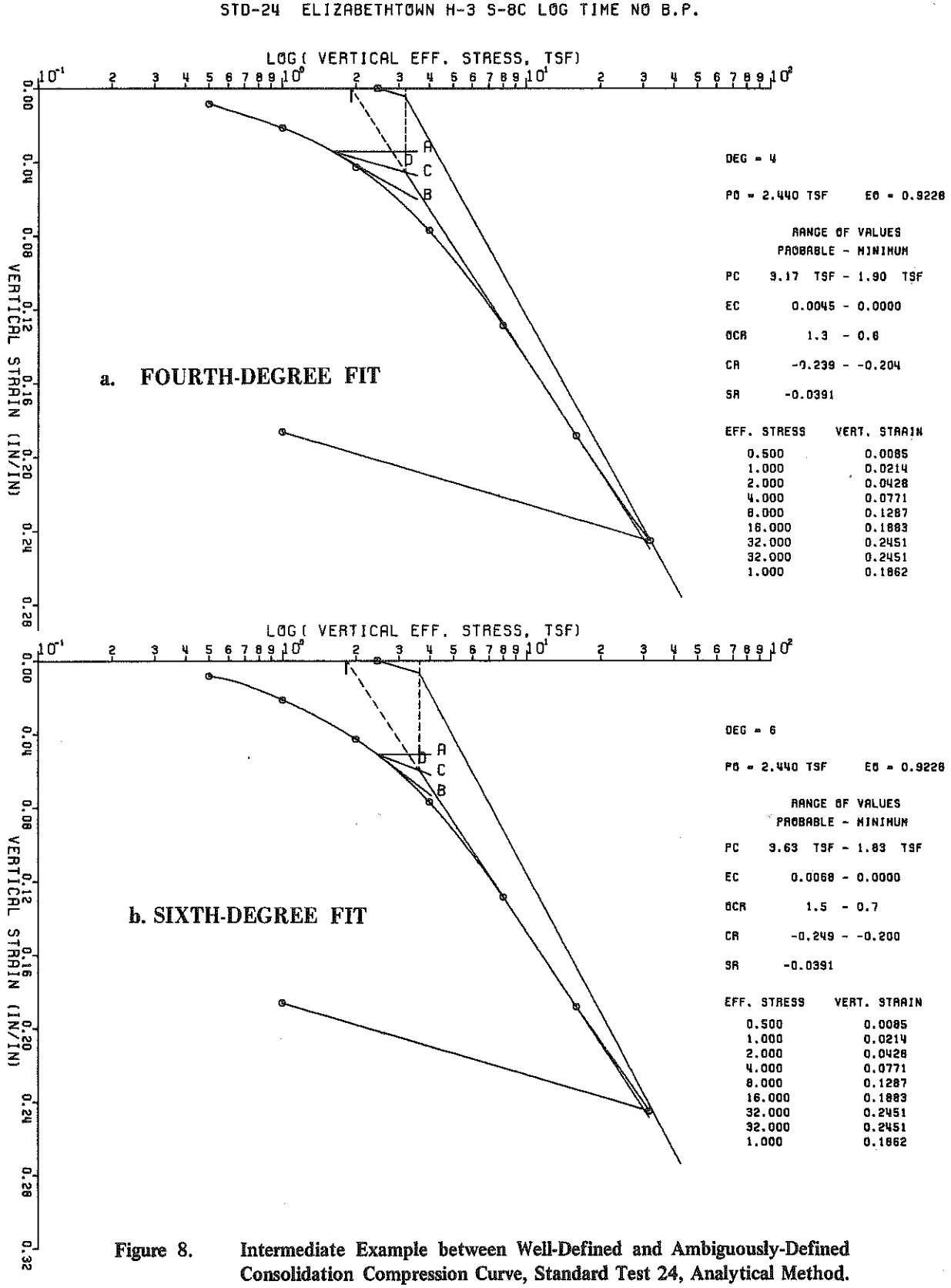

Figure 8. **Intermediate Example between Well-Defined and Ambiguously-Defined Consolidation Compression Curve, Standard Test 24, Analytical Method.**

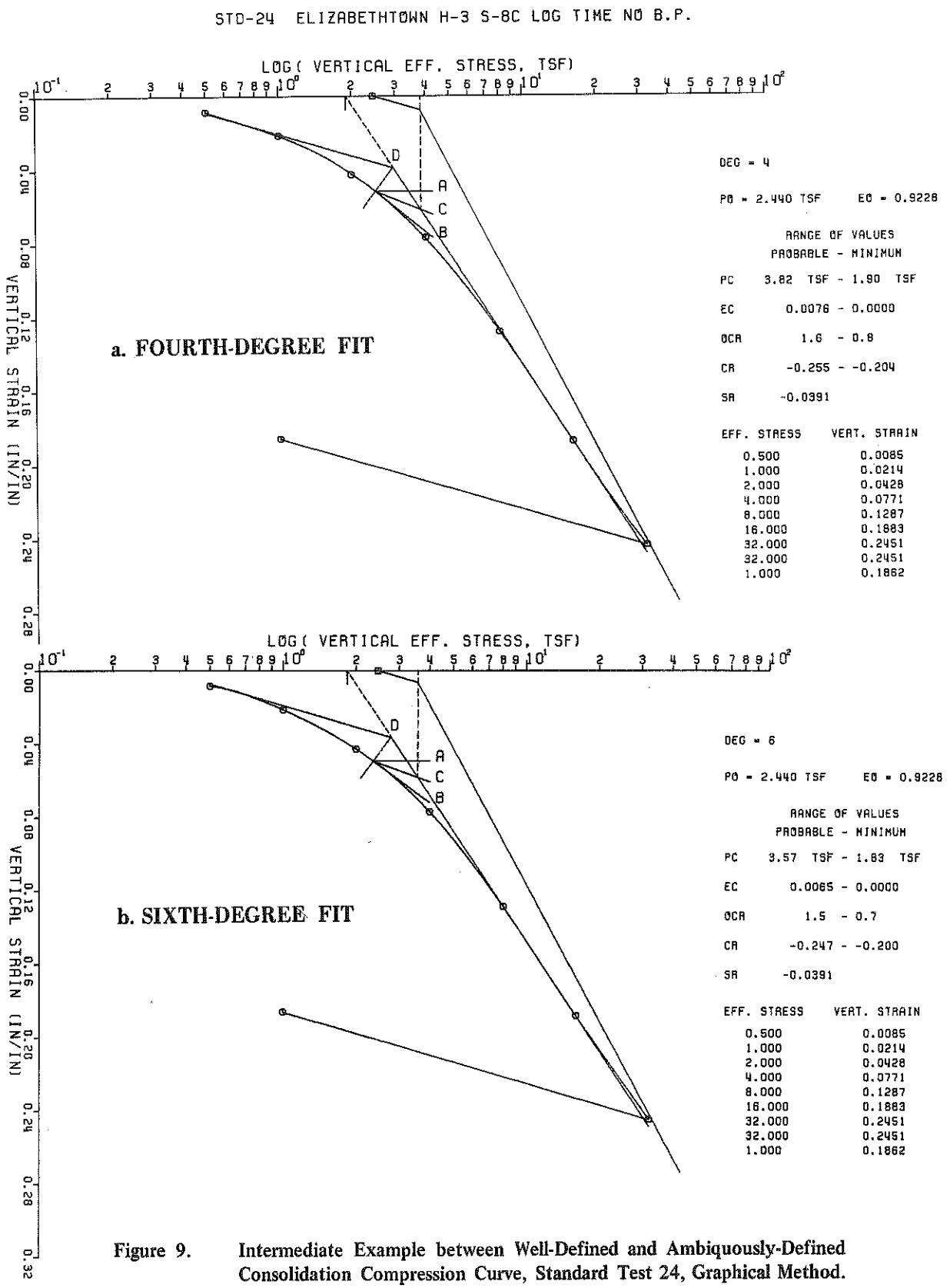

Figure 9. Intermediate Example between Well-Defined and Ambiquously-Defined Consolidation Compression Curve, Standard Test 24, Graphical Method.

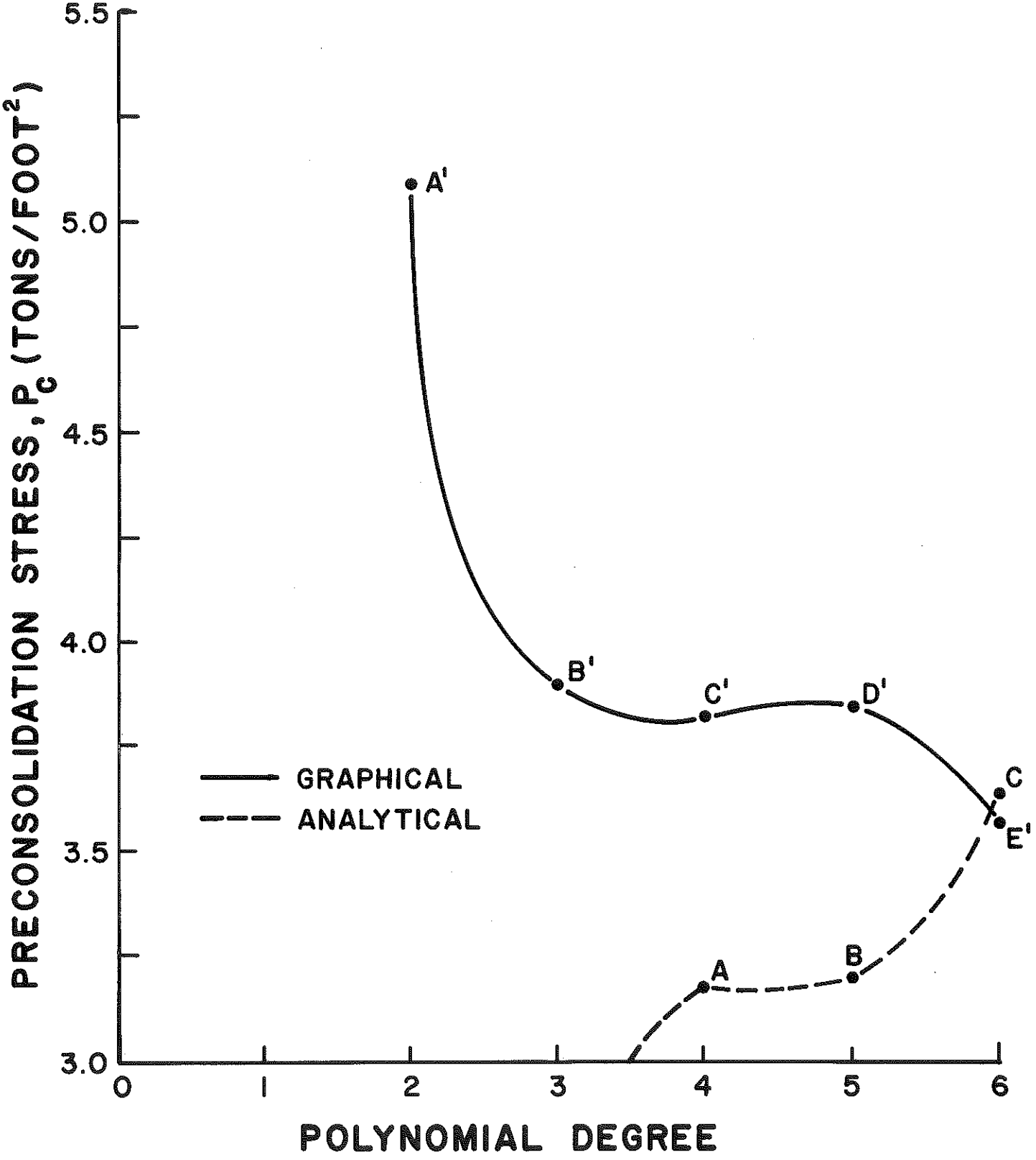

Figure 10. Preconsolidation Stress versus Polynomial Degree, Standard Test 24.

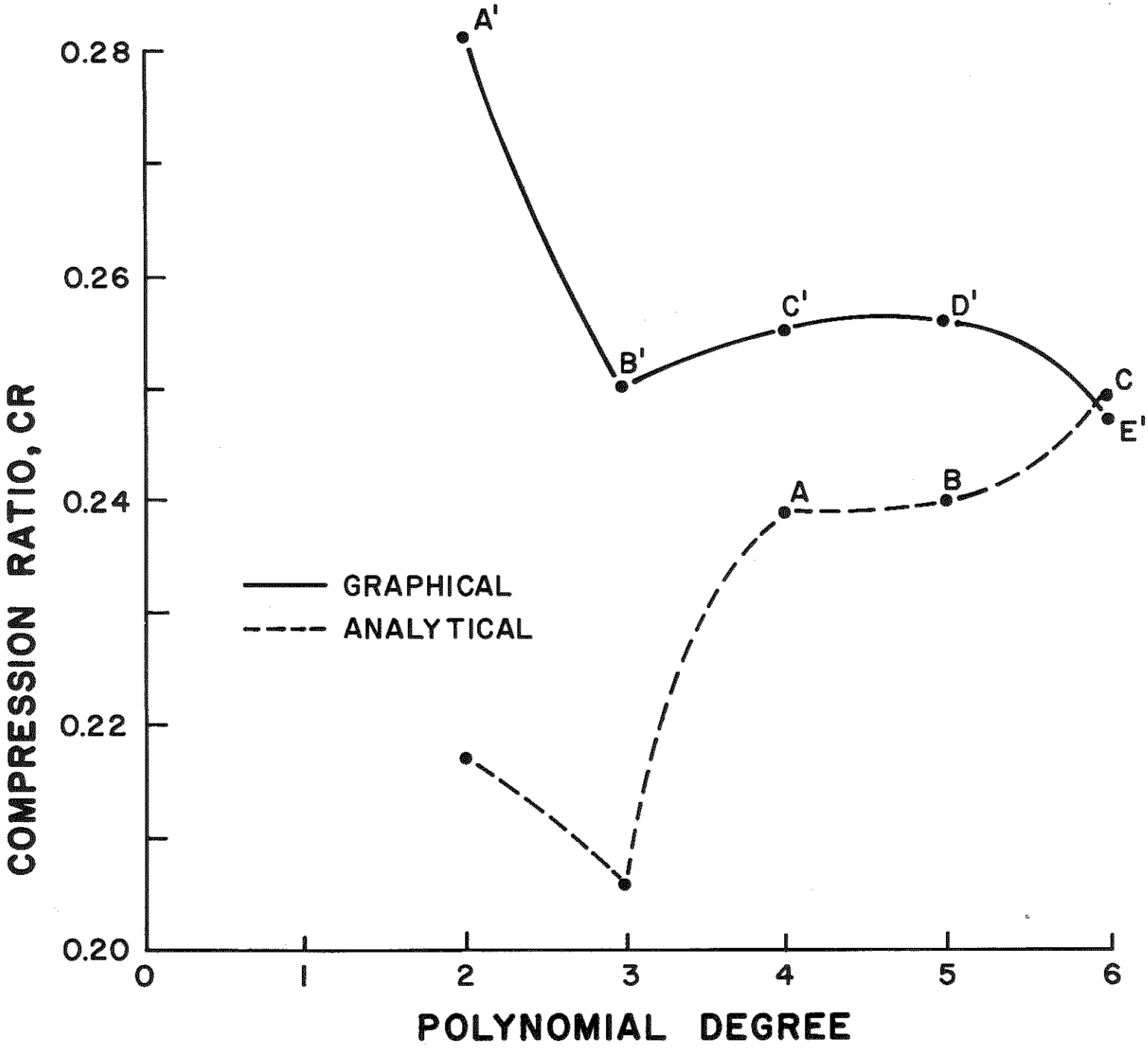

Figure 11. Compression Ratio versus Polynomial Degree, Standard Test 24.

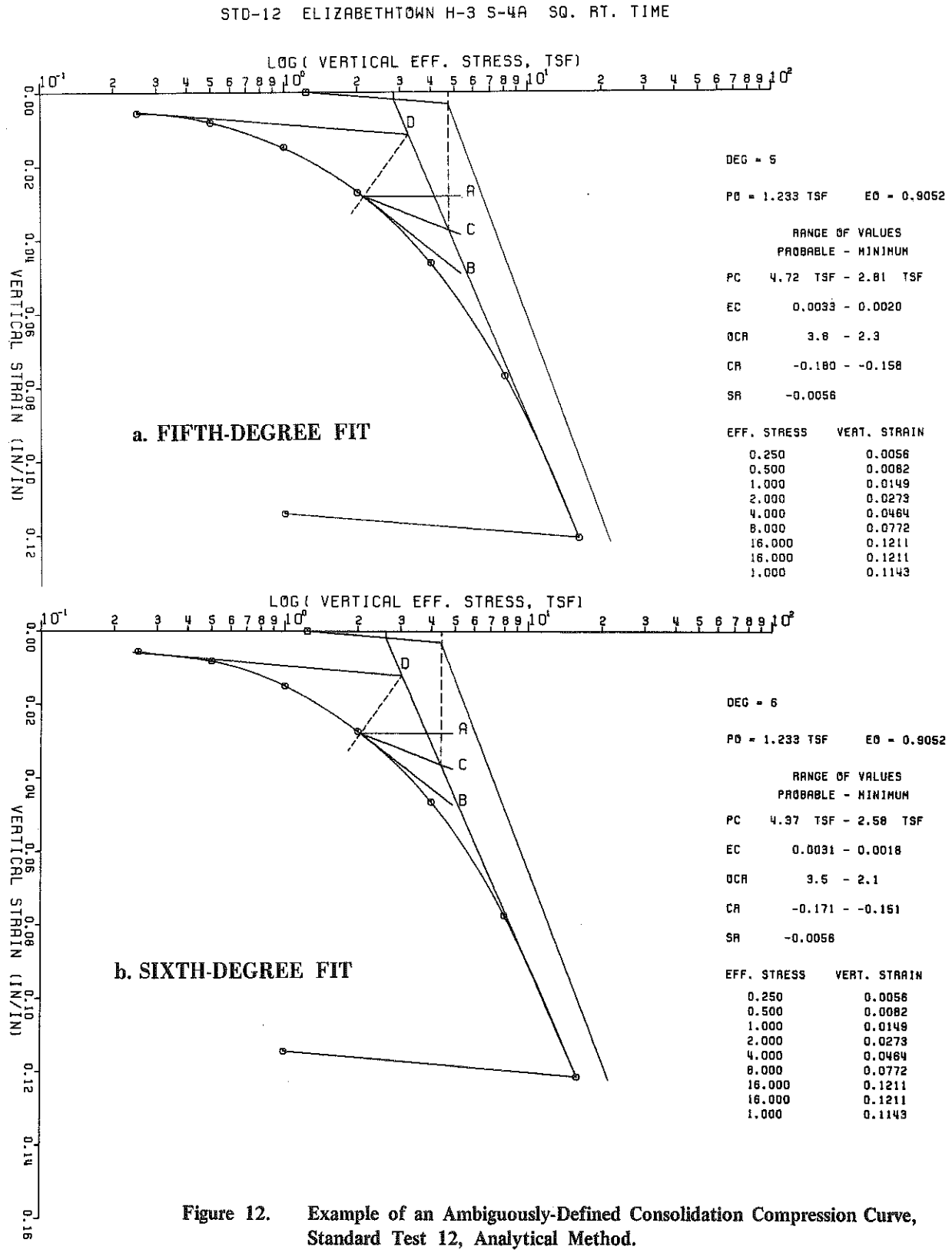

Figure 12. **Example of an Ambiguously-Defined Consolidation Compression Curve, Standard Test 12, Analytical Method.**

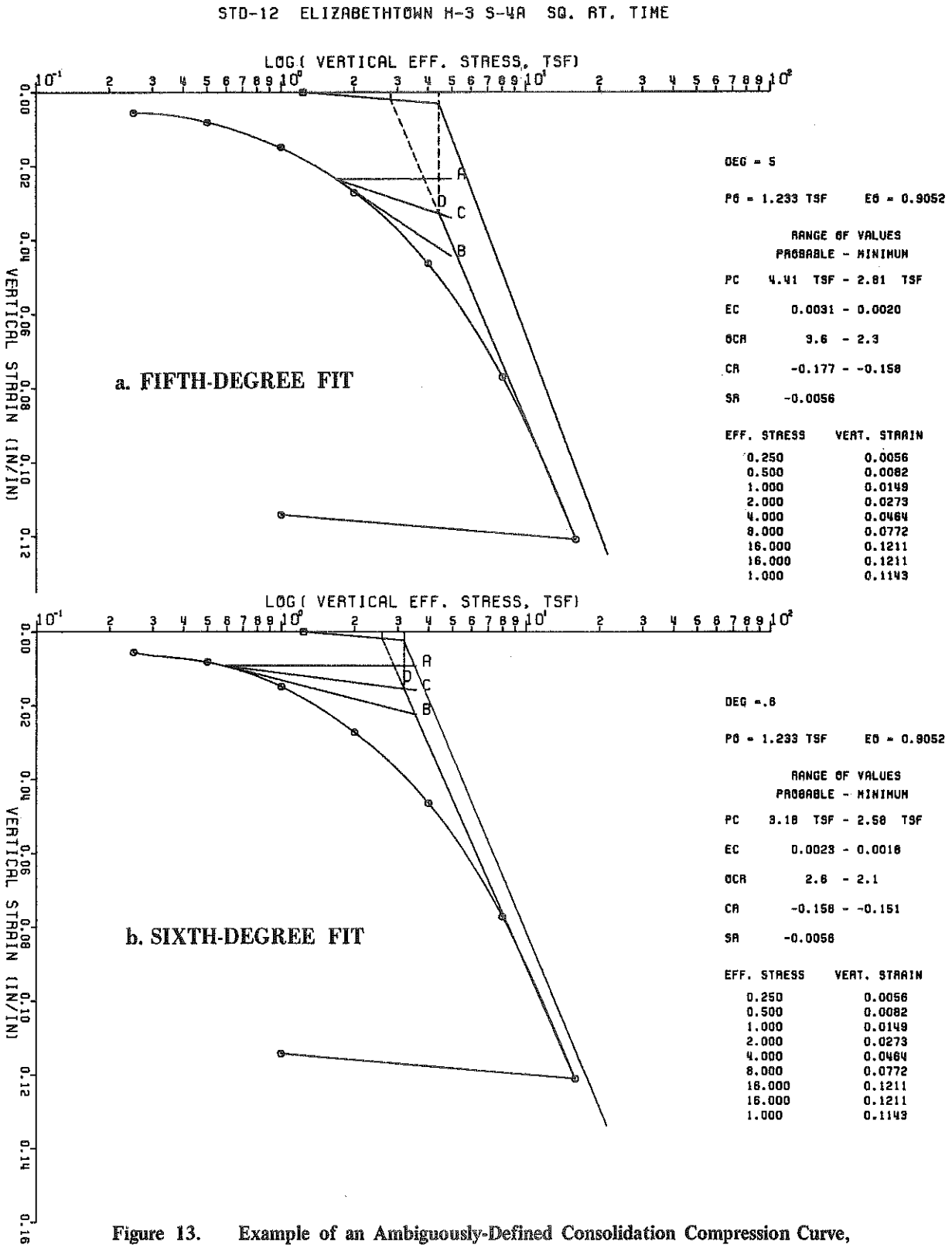

Figure 13. Example of an Ambiguously-Defined Consolidation Compression Curve, Standard Test 12, Graphical Method.

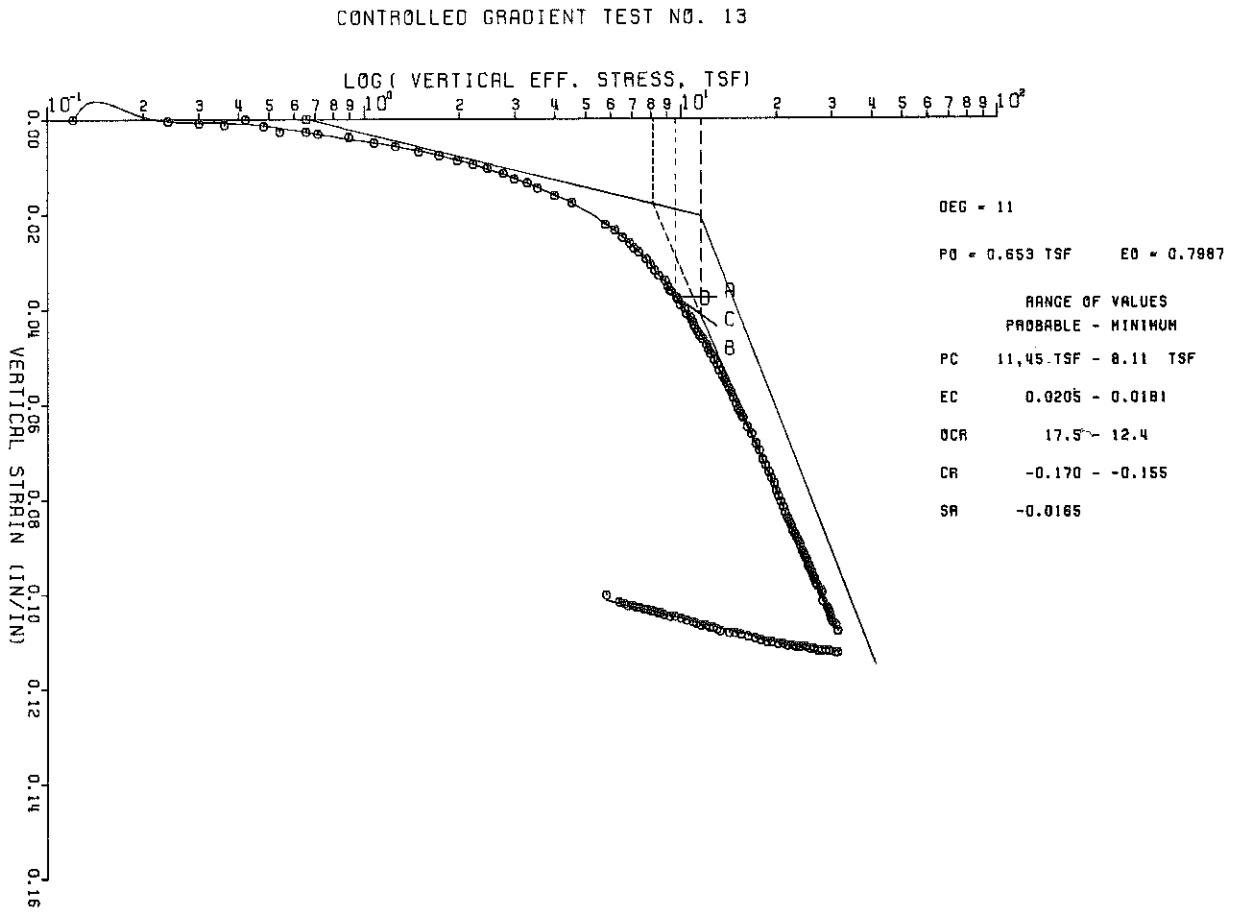

Figure 14. Selection of Point of Maximum Curvature Using Equation 3.

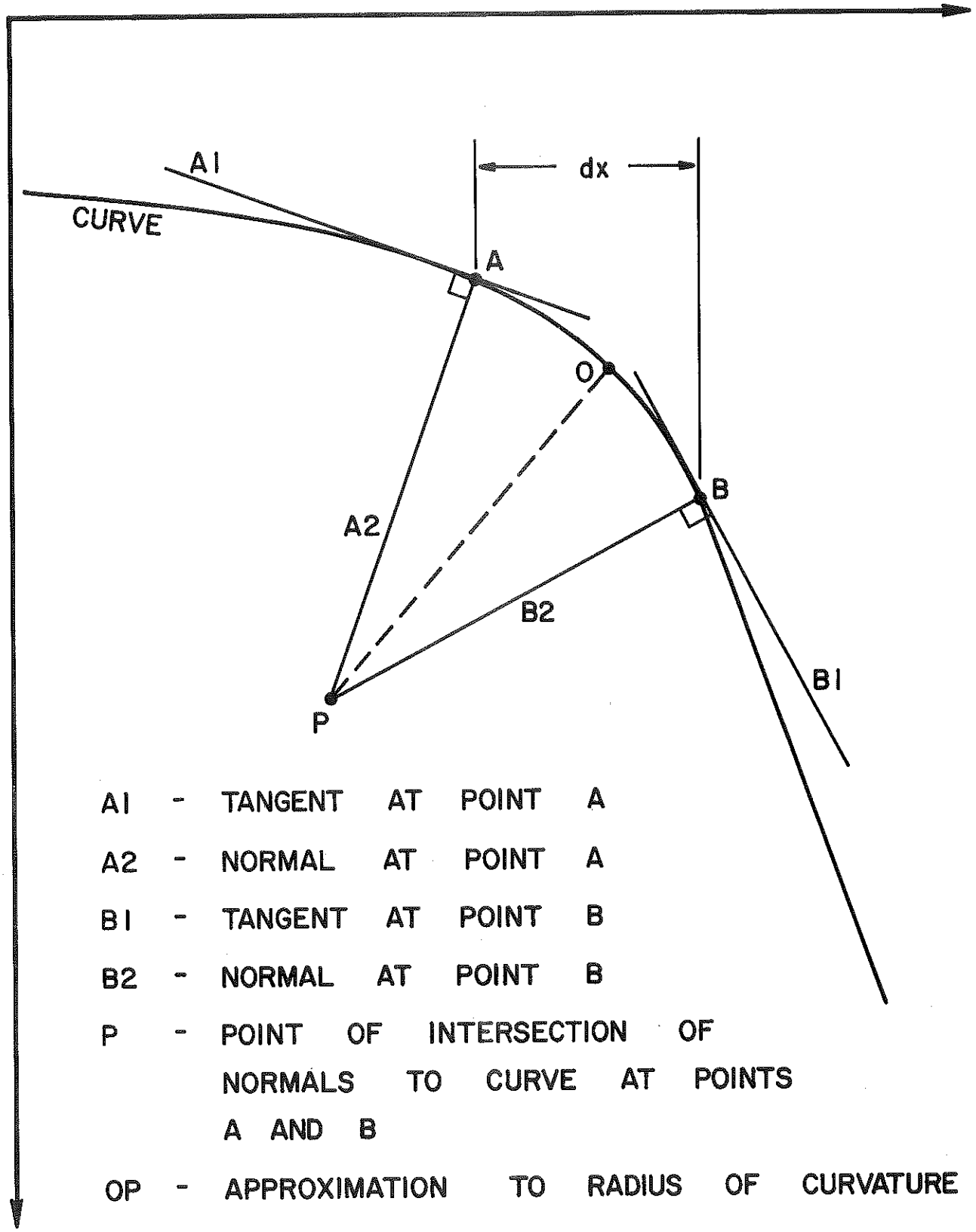

Figure 15. Geometrical Determination of Point of Maximum Curvature.

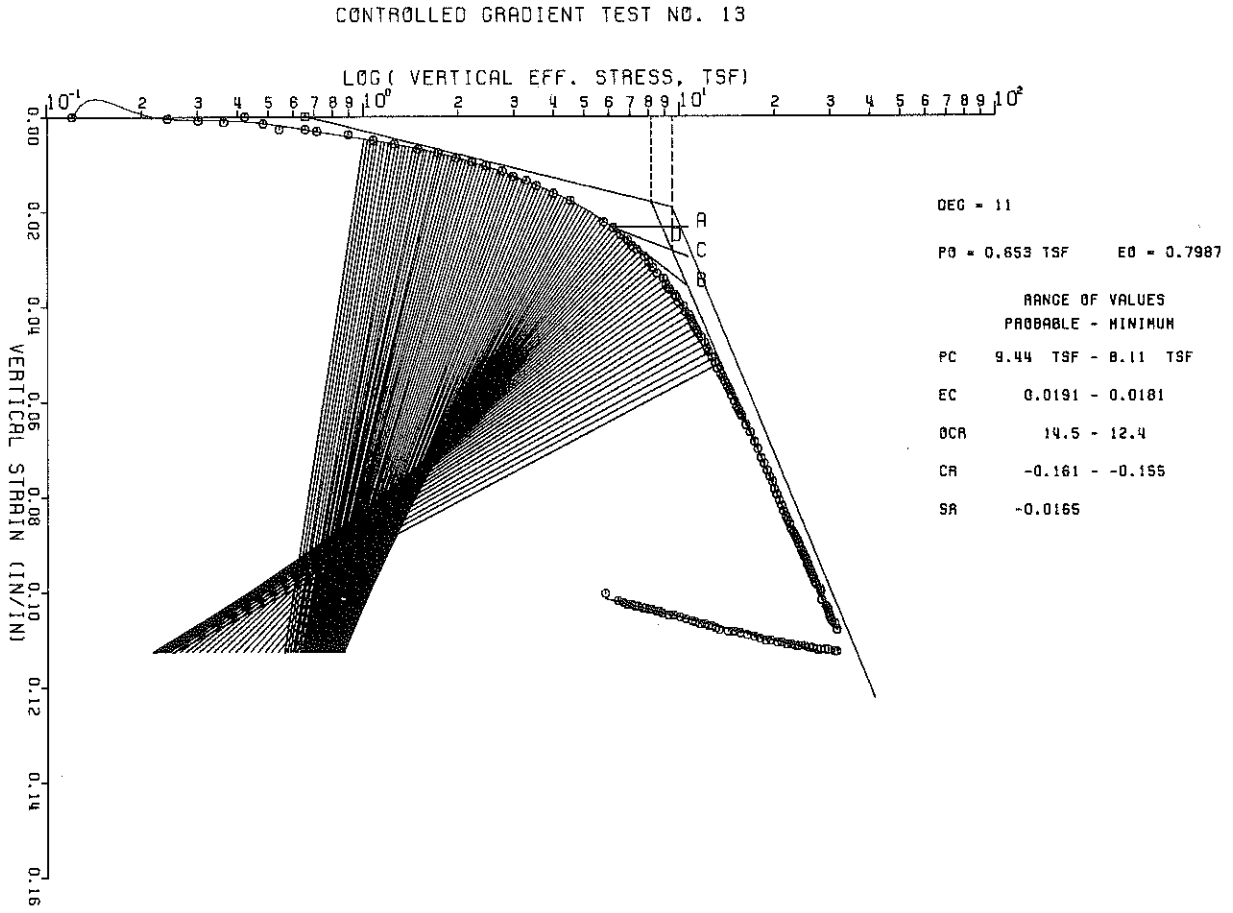

Figure 16. **Computerized Operation of Geometrical Determination of Radius of Curvature.**

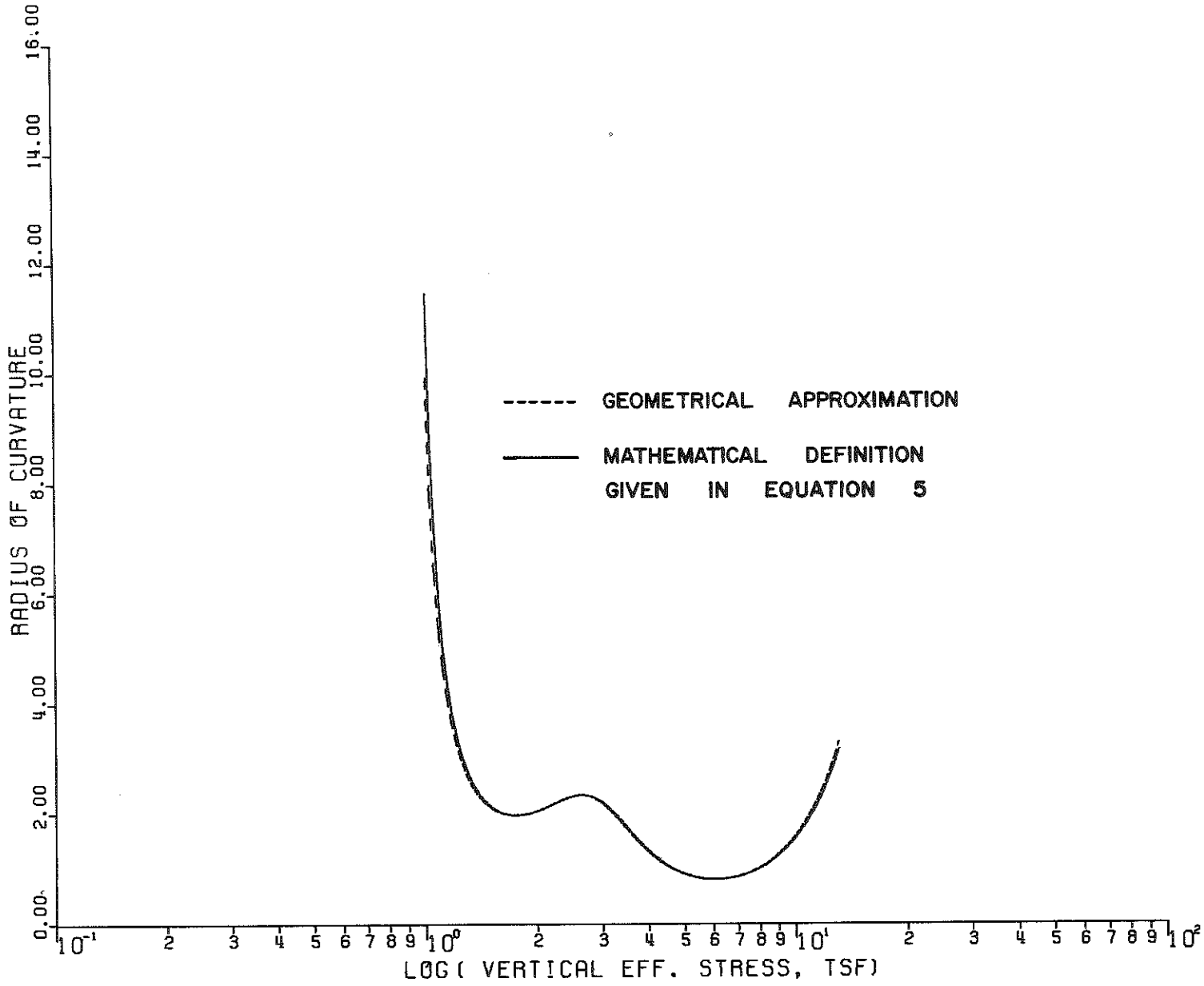

Figure 17. **Comparison of Values of Radius of Curvature as Determined by Geometrical Approach and Equation 5.**